ELSEVIER

Journal of Photochemistry and Photobiology A: Chemistry 116 (1998) 27–37

Journal of Photochemistry and Photobiology A:Chemistry

Charge-transfer effects on the fluorescence spectra of 9-aminocamptothecin Steady-state and time-resolved fluorescence studies

Joykrishna Dey, Isiah M. Warner *

Department of Chemistry, Louisiana State University, Baton Rouge, LA 70803, USA

Received 22 October 1997; received in revised form 9 March 1998; accepted 26 March 1998

Abstract

The steady-state and time-resolved fluorescence of 9-amino-20 (*S*)-camptothecin (ACAM) were measured in a series of organic solvents. The molecule exhibits charge-transfer (CT) fluorescence in nonhydrogen-bonding polar solvents. The solvatochromic data have been utilized to estimate the dipole moment of the molecule in the lowest excited singlet state. The CT fluorescence of ACAM is quenched in polar and hydrogen-bonding solvents. The fluorescence quenching of ACAM by methanol, water, and 2,2,2-trifluoroethanol were studied in 1,4-dioxane. The quenching efficiency is linearly related to hydrogen bond-donating capacity of the quencher molecule. Semiempirical AM1 molecular orbital calculations have been performed to calculate excitation energies, oscillator strengths, and ground and excited-state dipole moments of ACAM as well of the parent drug, camptothecin.

Keywords: 9-Aminocamptothecin; Fluorescence spectra; Solvent effect; Fluorescence lifetime; Fluorescence quenching; Excited-state dipole moment; Molecular orbital calculations

1. Introduction

The 9-amino-20 (*S*)-camptothecin, ACAM (I) (Fig. 1) is an anticancer drug currently under phase I clinical trials in the USA [1]. The parent drug, 20 (*S*)-camptothecin, CAM (II) (Fig. 1) a plant alkaloid was first isolated and characterized by Wall et al. [2] in 1966 from a Chinese tree *Camptotheca acuminata* (family Nyssaceae). This pentacyclic alkaloid contains a quinoline ring system (ring A and B), a pyridone ring (ring D) and a terminal α-hydroxy lactone ring (ring E). It has a chiral center (C-20) within the lactone ring. Following its discovery and chemical identification, CAM was found to be active in tests against L1210 leukemia [3] and Walker 256 carcinosarcoma [2,4,5]. It was also found that CAM inhibits both DNA and RNA synthesis in mammalian cells. This attracted immediate interest in CAM as a potential cancer chemotherapeutic agent. Its high antitumor activity against a wide range of experimental tumors has been confirmed [6]. The CAM was clinically evaluated as its water-soluble sodium salt due to its poor aqueous solubility. Several water-soluble CAM analogs were also synthesized [7] and clinically evaluated [8]. However, only 9-, 10-, and 11-substituted derivatives have shown anticancer activity in a number of in vitro and in vivo studies [9–16]. The results of preclinical and clinical developments of CAM and its analogs have been reviewed in two recent reports [17,18].

In most studies reported so far, attention has been mainly focused on the structure-activity relationship (SAR) of CAM and its synthetic analogs. Burke et al., in a series of publications, have reported the binding of the parent drug as well as its analogs with human serum albumin and lipid bilayers. These bindings were confirmed by exploiting the fluorescence properties of CAM and its analogs [19–24]. However, to our knowledge, there has not been a report on the detailed fluorescence spectral and photophysical studies of these drugs except for a few scattered studies [1,19–24]. Therefore, we have undertaken a systematic study of the electronic absorption and fluorescence spectral properties of CAM and its analogs. Recently, we have reported the fluorescence spectral behavior, and ground and excited-state proton-transfer properties of CAM in organic solvents and in aqueous solutions [25,26]. Burke et al. [1] used the pH sensitive fluorescence of ACAM to estimate its binding constant with phospholipid vesicles. They reported that the fluorescence intensity of ACAM increases upon decrease of pH as a result of protonation at the amine group. In such a case,

* Corresponding author.

1010-6030/98/$ - see front matter
PII S1010-6030(98)00280-9

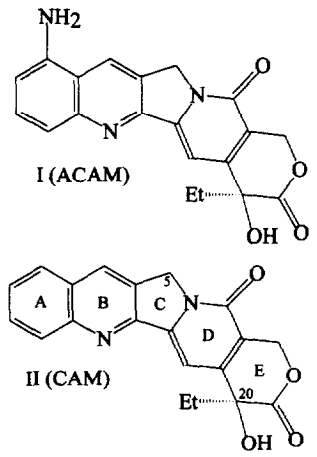

Fig. 1. Structures of 9-amino-20 (*S*)-camptothecin (I) and 20 (*S*)-camptothecin (II).

one would expect the resulting fluorescence spectrum to resemble the fluorescence spectrum of the neutral form of CAM in water. However, the spectrum reported in the paper showed an emission band which is red-shifted relative to that of the neutral CAM molecule. In order to understand the spectral behavior of ACAM, we have studied in detail the electronic absorption and fluorescence spectra of ACAM in various environments. A report on the pH effect on absorption and fluorescence spectra of the molecule will appear in a separate publication. In the present work, we discuss the effects of organic solvents on the fluorescence spectral behavior and photophysical properties of 9-aminocamptothecin.

2. Experimental

2.1. Materials

The 9-amino-20 (*S*)-camptothecin (Lot # 94B10A) was a gift from Pharmacia. The sample was 99.9% pure as reported by Pharmacia and was used without further purification. Spectroscopic grade cyclohexane (Aldrich), 1,4-dioxane (Aldrich), tetrahydrofuran (Mallinckrodt), ethyl acetate (Mallinckrodt), 1,2-dimethoxyethane (Aldrich), dichloromethane (Aldrich), chloroform (Aldrich), acetonitrile (Aldrich), dimethylformamide (Mallinckrodt), dimethylsulfoxide (Mallinckrodt), methanol (Aldrich), ethanol (Aldrich), propanol (Mallinckrodt), butanol (Mallinckrodt), and ethylene glycol (Aldrich) were used as received. Deionized distilled water was used for making aqueous solutions.

2.2. Methods

A stock solution of ACAM ($\sim 10^{-3}$ M) was made in 1,2-dimethoxyethane. An aliquot of this solution was taken in a flask and the solvent was evaporated to dryness by slow purging of dry nitrogen gas. The appropriate solvent was then added to make final solution. For quenching studies, dilute solutions of ACAM ($\sim 10^{-4}$ M) and quencher (~ 1 M) were made in dioxane. Fluorescence quantum yields, Φ_f, were determined according to the method of Parker and Rees [27] in reference to quinine sulfate in 0.1 N H_2SO_4 ($\Phi_f = 0.545$) [28,29]. The absorbance of the solutions including quinine sulfate at the wavelength of excitation (360 nm) was maintained at < 0.05. Theoretical calculations were performed using the semiempirical AM1 method [30]. The molecular geometry was preoptimized using Tripos SYBYL 5.2 forcefield before AM1 calculations.

2.3. Apparatus

The absorption spectra were measured on a double beam Shimadzu UV-3101PC spectrophotometer equipped with a constant temperature circulator. The fluorescence spectra were measured on a Spex-Fluorolog model F2T21I spectrofluorometer equipped with a cell compartment thermostated with a VWR model 1160 constant temperature circulator. The band pass of the excitation and emission monochromators were set at 5 and 3.4 nm, respectively. Fluorescence lifetimes were measured on a PTI LS-100 luminescence spectrometer. The 358 nm emission of N_2 was used for sample excitation. The decay curves were obtained by use of the time correlated single photon counting (TC-SPC) technique. The data were analyzed by using a multiexponential decay analysis program. All measurements were conducted at 25°C unless otherwise mentioned.

3. Results

3.1. Absorption spectra

The absorption spectra of ACAM were measured in a series of organic solvents. The spectral data appear in Table 1. A representative absorption spectrum of the molecule in acetonitrile is depicted in Fig. 2. For comparison purposes, the absorption spectrum of the parent drug in the same solvent has also been included in the figure. The absorption spectrum of ACAM is very similar to that of CAM, except the short-wavelength band is red-shifted relative to the corresponding band of the latter. Also, a new band ($\lambda_{max} \sim 335$ nm) appears on the higher energy side of the long-wavelength band. Upon protonation at the amine group the band disappears and the resulting absorption spectrum (not shown here) resembles that of CAM [26]. The lowest energy absorption bands of ACAM are relatively insensitive to solvent polarity. However, in protic solvents, the long-wavelength absorption bands are slightly red-shifted.

3.2. Steady-state fluorescence measurements

The fluorescence spectra of ACAM in some selected aprotic and protic solvents are displayed in Figs. 3 and 4, respectively. The most notable feature of the fluorescence

Table 1
Solvent polarity parameters ($F(\varepsilon,n)$), absorption and fluorescence maxima [λ_{max}(abs) and λ_{max} (flu), respectively], fluorescence quantum yields (Φ_f) and lifetimes (τ_f) of ACAM in organic solvents

No.	Solvent	$F(\varepsilon,n)$[a]	λ_{max} (abs) (nm)	λ_{max} (flu) (nm)	Φ_f ($\pm$0.001)	τ_f[b] ($\pm$0.2 ns)
1	Cyclohexane	0.000	365 338 263	480 424	–	–
2	1,4-Dioxane	0.021	365 337 263	533 428	0.129	15.5 (3.8, 0.8)
3	Ethyl acetate	0.200	363 338	525 426	0.035	7.6 (4.5, 2.2)
4	1,2-Dimethoxyethane	0.215	364 335 262	540 427	0.040	6.8, 4.4 (3.5, 1.3)
5	Acetone	0.285	363 337	547 428	0.029	11.6, 3.7, 1.6 (4.0, 1.0)
6	Dimethylformamide	0.275	365 339	547 431	0.015	8.4, 2.6 (7.2, 1.3)
7	Dimethylsulfoxide	0.264	361 343	561 434	0.008	5.6, 1.7 (6.4, 1.7)
8	Acetonitrile	0.306	362 335 262	552 427	0.022	10.2, 2.9 (5.4, 1.4)
9	Propylene carbonate	–	367 335 262	542 429	0.024	8.7, 1.9 (6.4, 1.9)
10	*n*-Butylchloride	0.210	365 332 262	530 425	0.82	14.0 (3.5, 0.7)
11	Chloroform	0.149	363 335 263	521 426	0.400	16.9 (3.4, 0.8)
12	Dichloromethane	0.218	363 335 262	533 427	0.114	17.9 (4.7, 2.6)
13	Tetrahydrofuran	0.210	364 335	536 428	–	6.5 (4.1, 1.1)
14	Methanol	0.309	367 338 265	432	0.003	6.9, 4.3, 1.0
15	Ethanol	0.289	369 338 265	553(s) 462 433	0.004	7.2, 0.9 (8.4, 4.2, 1.0)
16	*n*-Propanol	0.275	367 360 337 263	550(s) 471 436	0.004	8.6, 1.4 (4.2, 0.9)
17	*n*-Butanol	0.264	369 335 263	547 476 434	0.006	9.7, 2.3 (4.0, 1.5)
18	Ethylene glycol	0.275	372 336 264	550(s) 434	0.003	7.2, 1.2 (5.6, 3.0)
19	Water (pH 5.2)	0.320	366 337 265	434	0.004	4.7

[a]The values were calculated using ε and n values of the respective solvents obtained from Ref. [31].
[b]The values within the parentheses represent fluorescence decay times corresponding to short-wavelength emission band.

spectra of ACAM is that a large Stokes-shifted band exists in addition to a short-wavelength (SW) band in the solvents employed. Note that the fluorescence spectral profiles are solvent dependent. In particular, the long-wavelength (LW) emission is absent in water. The feature and the position of the SW band is very similar to that of CAM in the same

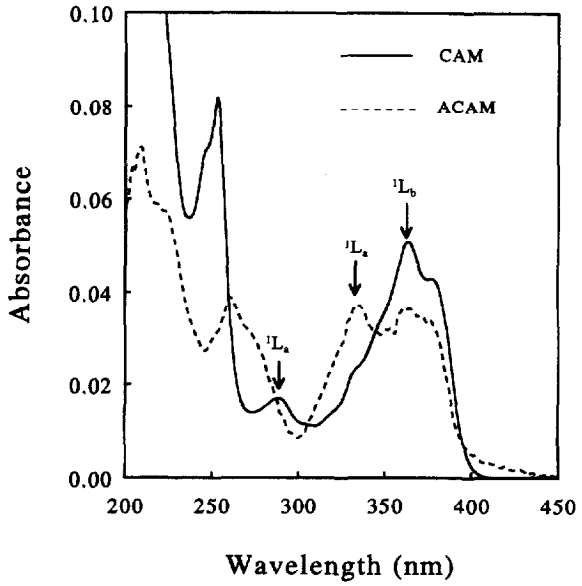

Fig. 2. Absorption spectra of ACAM and CAM in acetonitrile.

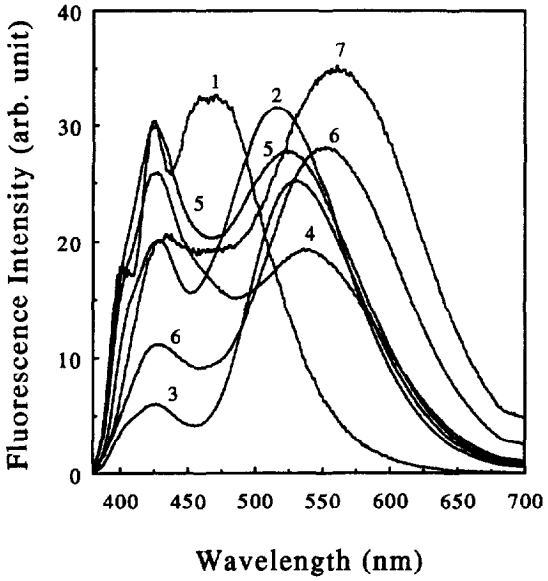

Fig. 3. Fluorescence spectra of ACAM in aprotic organic solvents: (1) cyclohexane, (2) 1,4-dioxane, (3) dichloromethane, (4) 1,2-dimethoxyethane, (5) ethyl acetate, (6) acetonitrile, (7) dimethylsulfoxide.

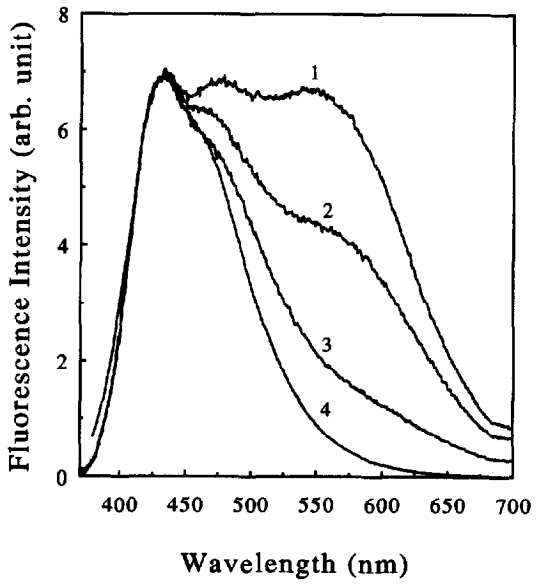

Fig. 4. Fluorescence spectra of ACAM in protic solvents: (1) *n*-butanol, (2) *n*-propanol, (3) methanol, (4) water.

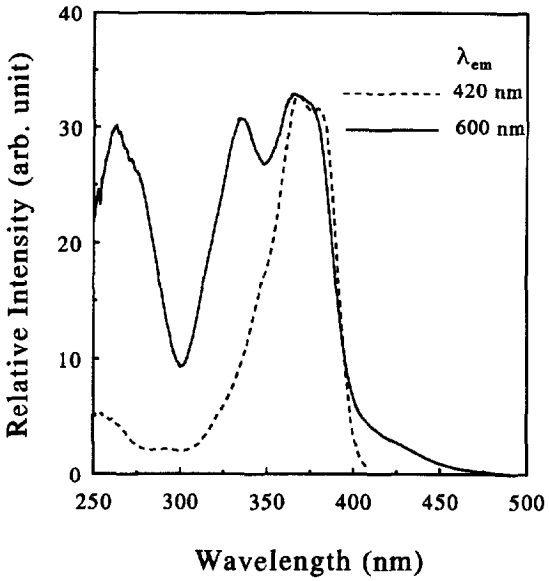

Fig. 5. Fluorescence excitation spectra of ACAM in acetonitrile.

solvent [25]. The fluorescence excitation spectra (Fig. 5) of the respective emission bands of ACAM measured in acetonitrile solvent are different from each other. The excitation spectrum corresponding to the LW band resembles the absorption spectrum of ACAM. However, the excitation spectrum for the SW band resembles the absorption spectrum of the parent drug, CAM. Also, the fluorescence excitation spectra (not shown here) measured at different emission wavelengths of the SW band of ACAM in water, in which the LW band is absent, are similar to each other and closely resemble the absorption spectrum of CAM in water.

Although the lowest energy absorption bands of ACAM are insensitive to solvent polarity, the fluorescence spectra are highly solvatochromic. This is noted in Fig. 3 where the fluorescence spectra in aprotic solvents varies with polarity. The data in Table 1 indicate that the emission maximum of the LW band shifts to the red with an increase in solvent polarity. The polarity-dependent shift of the emission maximum can be seen in Fig. 6, which shows the fluorescence spectra of ACAM in dioxane containing various concentrations of acetonitile (ACN). Clearly, as the % of acetonitrile increases, the fluorescence intensity of the LW band is observed to decrease and is accompanied by a large red shift of the band maximum. A plot of λ_{max} as a function of concentration of acetonitrile is shown in Fig. 7. The relevant data are listed in Table 2. The solvatochromic shifts in pure solvents have been correlated with the solvent polarity parameter, $F(\varepsilon,n)$ [31] following the Lippert–Mataga equation [id[ef,33]:

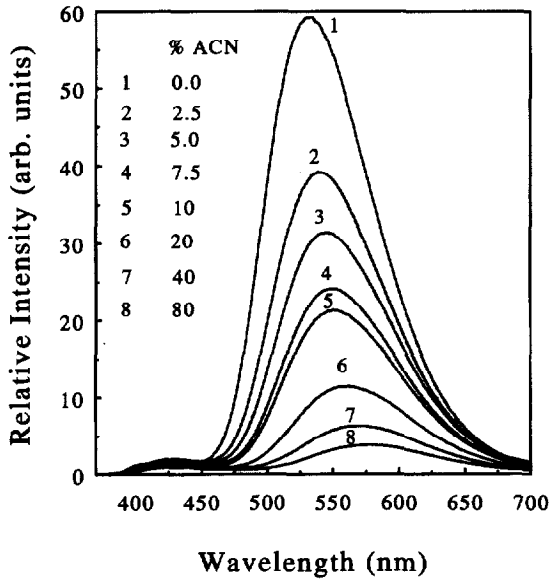

Fig. 6. Fluorescence spectra of ACAM in dioxane containing various % (v/v) of acetonitrile.

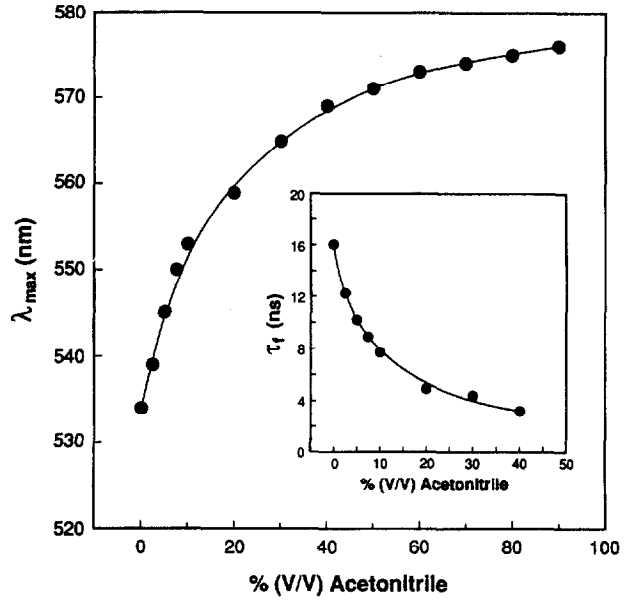

Fig. 7. Plot of emission maxima of ACAM (λ_{max}) as a function of % (v/v) acetonitrile; (insert) plot of fluorescence lifetime (τ_f) vs. % (v/v) acetonitrile.

$$\Delta\nu_s = \frac{2(\mu^* - \mu)^2}{hca^3} F(\varepsilon,n) + \text{Const.}$$

$$F(\varepsilon,n) = \frac{\varepsilon - 1}{2\varepsilon + 1} - \frac{n^2 - 1}{2n^2 + 1}$$

where $(\mu^* - \mu)$ is the difference between the excited and ground-state dipole moments, 'a' is the Onsager cavity radius, ε and 'n' are the dielectric constant and refractive index of the solvent, respectively. Fig. 8 shows a plot of Stokes shifts ($\Delta\nu_s$, in cm^{-1}) of the LW band in neat organic solvents against the solvent polarity function. The Stokes shifts correlate linearly with the polarity parameter, except

Table 2
Fluorescence maxima (λ_{max}) and lifetimes (τ_f) of ACAM in dioxane containing various % (v/v) of acetonitrile

% (v/v) Acetonitrile	λ_{max} (nm)	τ_f (ns)
0.0	534	16.0
2.5	539	12.2
5.0	545	10.2
7.5	550	8.9
10	554	7.7
20	559	4.9
30	565	4.4
40	569	3.2
50	571	–
60	573	–
70	574	–
80	576	–
90	578	–

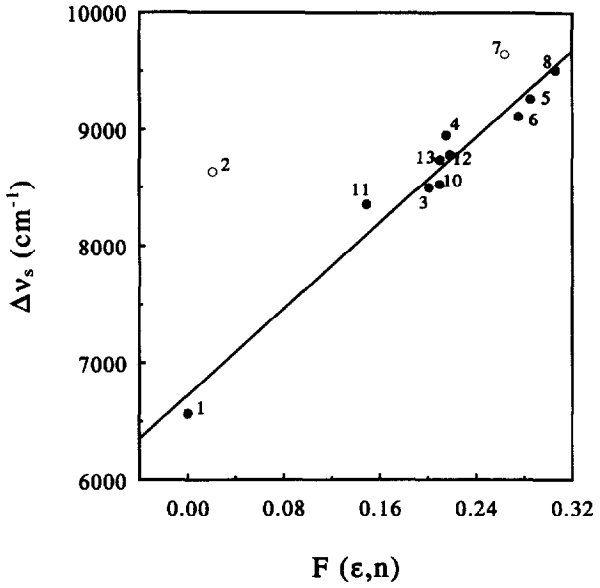

Fig. 8. Plot of Stokes shift ($\Delta\nu_s$) vs. polarity parameter $F(\varepsilon,n)$; the data points corresponding to dioxane and dimethylsulfoxide solvents were not included in the curve fitting.

for solvents, e.g., dioxane (2) and dimethylsulfoxide (7). The slope of the plot suggests a large change in dipole moment of the molecule upon electronic excitation and hence a strong CT character of the emitting state. The dipole moment of the molecule in the excited state can be obtained from the slope (9232 cm^{-1}) of the Lippert–Mataga plot. Assuming a equal to 6.38 Å (which is estimated from the optimized distance (12.76 Å) between two farthest atoms of the molecule in the direction of charge separation), we obtained $\Delta\mu$ $(=\mu^* - \mu)$ equal to 15 D. The ground-state dipole moment (μ) of the molecule obtained from AM1 calculation is 7.09 D which is consistent with the calculated ground-state dipole moment of CAM (7.1 D) [34]. From the calculated ground-state dipole moment value, the excited-state dipole moment (μ^*) of ACAM was obtained as equal to 22.09 D. This is however, much higher than the calculated

dipole moment (13.89 D) for the S_2 state. This large difference is probably due to the overestimation of a, the 'Onsager cavity radius'.

In protic solvents, the intensity of the LW emission decreases as the hydrogen bond-donating capacity of the solvent increases in going from butanol to water (see Fig. 4). In fact, the LW band completely disappears in water. To examine the effects of hydrogen-bonding interaction with the solvent molecules, we have measured fluorescence spectra of ACAM in dioxane solvent in the presence of low concentrations of methanol, water, and trifluoroethanol (TFE). Fig. 9 displays the fluorescence spectra of ACAM in dioxane in the presence of various concentrations of water. As noted, the fluorescence intensity of the LW emission band decreases as the water concentration increased. The decreased fluorescence intensity is also accompanied by a red shift of the emission maximum. The fluorescence spectrum shifts to longer wavelength by 16 nm in the presence of 0.5 M water in dioxane. Similar spectral changes were also observed upon addition of methanol and TFE. The emission maxima are listed in Table 3. The Stern–Volmer (S–V) plots for the steady-state fluorescence quenching of ACAM are shown in Fig. 10. The plots, except for water are linear. The S–V constant for TFE (8.98 M^{-1}) is higher than that for water (3.82 M^{-1}) and methanol (2.75 M^{-1}). The nonlinearity of the S–V plot for water in Fig. 10 may be due to the effect of solvent polarity on the fluorescence intensity as discussed in the preceding paragraph.

The fluorescence quantum yield data are listed in Table 1. As seen, the Φ_f value decreases with an increase in dielectric constant and hydrogen-bonding capacity of the solvent. Although the polarity of dioxane is lower than the chlorinated hydrocarbons, the Φ_f values in the latter solvents are higher than that in the former. The polarity-dependent variation of fluorescence quantum yield is demonstrated in Fig. 6 which displays fluorescence spectra in dioxane containing various % of acetonitrile.

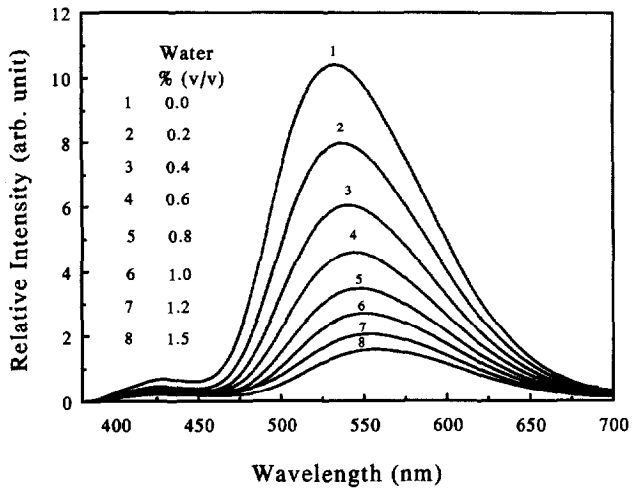

Fig. 9. Fluorescence spectra of ACAM in 1,4-dioxane in the presence of various concentrations of water.

Table 3
Fluorescence maxima (λ_{max}) and lifetimes (τ_f) of ACAM in dioxane containing varying concentration of methanol (MeOH), water, and 2,2,2-trifluoroethanol (TFE)

[Q]/M	MeOH		Water		TFE	
	λ_{max} (nm)	τ_f (ns)	λ_{max} (nm)	τ_f (ns)	λ_{max} (nm)	τ_f (ns)
0.0	553	15	534	15.1	533	15.0
0.05	536	12.6	535	12.5	536	10.8
0.10	537	10.2	538	10.9	538	7.5
0.15	537	8.5	540	9.5	539	6.4
0.20	539	7.1	541	8.5	542	5.4
0.25	549	6.4	543	8.0	544	4.7
0.30	541		545	7.2	546	4.3
0.35	543		546	6.7	547	3.4
0.40	544		546	5.8	548	3.2
0.45	544		548	5.5	550	3.0

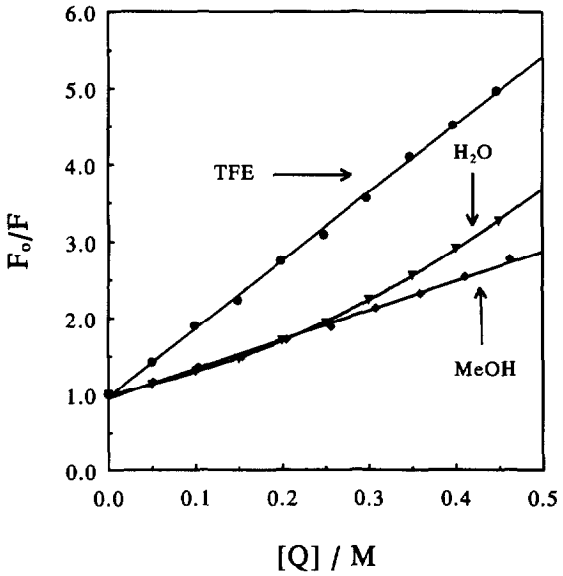

Fig. 10. Stern–Volmer plots for the steady-state fluorescence quenching of ACAM in dioxane by methanol (MeOH), water, and 2,2,2-trifluoroethanol (TFE).

3.3. Time-resolved fluorescence studies

The fluorescence lifetimes of ACAM have been measured in organic solvents employed in this study. The decay measurements were monitored at both SW (420 nm) and LW (550 nm) emission bands. The resulting fluorescence lifetime, τ_f, values appear in Table 1. The fluorescence decays at 550 nm are single exponential in aprotic and less polar solvents. However, the decays are biexponential in more polar and protic solvents. The fluorescence decays measured at the SW band are biexponential in all solvents used in this study. Of these, the τ_f value of the long-lived component corresponds to the lifetime of the parent drug, CAM. The τ_f values in nonpolar solvents, e.g., in dioxane, dichloromethane, and chloroform are very high. The data show that the τ_f value decreases in parallel with the Φ_f with an increase in solvent

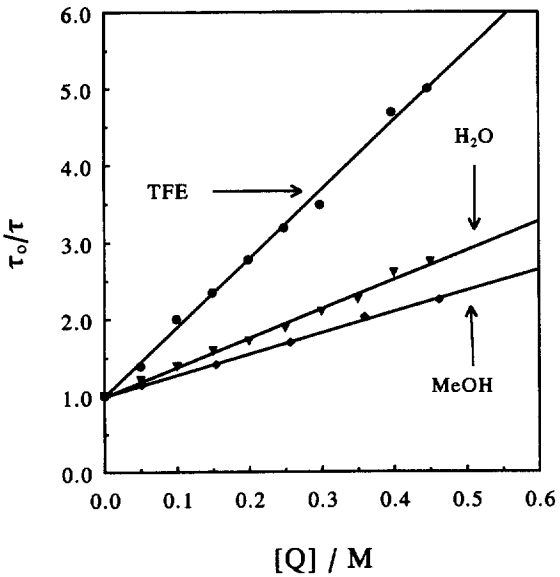

Fig. 11. Stern–Volmer plots for the time-resolved fluorescence quenching data of ACAM in dioxane by methanol (MeOH), water, and 2,2,2-trifluoroethanol (TFE).

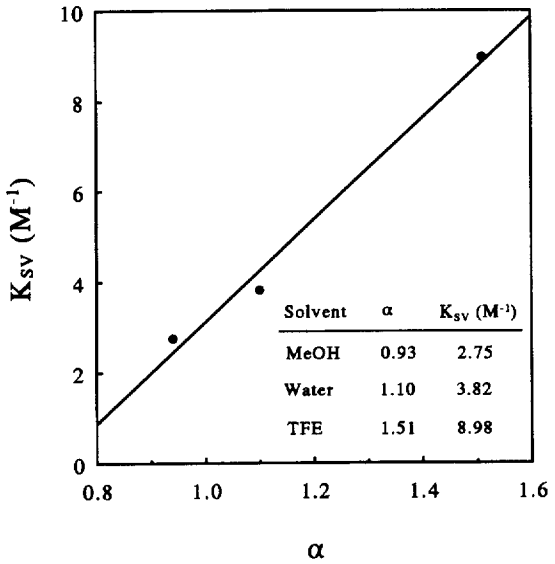

Fig. 12. Plot of Stern–Volmer constants (K_{SV}) as a function hydrogen-bond-donor acidity (α); (insert) list of α and K_{SV} values for different quenchers.

polarity and hydrogen-bonding capacity. To demonstrate the effect of solvent polarity, we have measured fluorescence decays of the LW emission in dioxane solvent containing various % (v/v) of acetonitrile. The data included in Table 2 clearly indicate a nonlinear (Fig. 7 (insert)) decrease of τ_f as the acetonitrile content of dioxane (i.e., polarity of the solvent) increases.

To examine the influence of hydrogen-bonding interaction with protic solvents in the excited state corresponding to the LW emission, we have measured fluorescence lifetimes (τ_f) of ACAM in dioxane in the presence of various concentrations of methanol, water, and TFE. A decrease in τ_f value can be observed from the data presented in Table 3 in the presence of increasing amounts of all three quenchers. The S–V plots constructed by use of the lifetime data are shown in Fig. 11. The Stern–Volmer constants (K_{SV}) obtained from the plots in Fig. 11 are almost identical within the experimental error with those obtained from the steady-state measurements (Fig. 10). The K_{SV} values are plotted against the hydrogen-bond-donor acidity (α) [35] of the quenchers in Fig. 12. The α values and the respective quenching constants are also included in this figure. The plot shows a linear correlation between the K_{SV} and α values.

3.4. Theoretical calculations

The quantum chemical molecular orbital (MO) calculations were performed for ACAM using the semiempirical AM1 method [36] to calculate the electronic spectra and dipole moments of the ground as well as excited states of the molecules. To compare the results, we have also done similar calculations for CAM. The molecular geometry was preoptimized first using MM+ force field[1] [37] and then by AM1 method before MO calculations were performed. A total of nineteen configurations involving three occupied and three unoccupied MOs were used for the calculations. The results are summarized in Table 4. The excitation energies are in good agreement with the corresponding experimental values. Interestingly, the $-NH_2$ substitution at the 9-position of CAM

[1] This is an extension of Allinger's MM2 force field. It uses the latest MM2 (1991) parameters and atom types with the 1977 functional form.

Table 4
Calculated electronic excitation energy, oscillator strength and state dipole moments of CAM and ACAM

CAM				ACAM			
Transition	Excitation energy (nm)	Oscillator strength	State dipole moment (D)	Transition	Excitation energy (nm)	Oscillator strength	State dipole moment (D)
S_o			7.100	S_o			7.089
$S_o \rightarrow S_1$	359.3	0.6808	7.873	$S_o \rightarrow S_1$	356.6	0.5955	7.958
$S_o \rightarrow S_2$	326.1	0.0112	9.609	$S_o \rightarrow S_2$	341.8	0.0313	13.883
$S_o \rightarrow S_3$	312.3	0.0955	9.473	$S_o \rightarrow S_3$	339.1	0.2895	11.766
$S_o \rightarrow S_4$	238.7	0.6558	3.192	$S_o \rightarrow S_4$	247.4	0.7412	5.474
$S_o \rightarrow S_5$	232.8	0.5504	5.619	$S_o \rightarrow S_5$	242.9	0.6949	6.477
$S_o \rightarrow S_6$	223.4	0.7076	6.943	$S_o \rightarrow S_6$	227.2	0.1618	4.326

does not change the position of the lowest energy transition. However, the short-wavelength transitions are shifted to longer wavelengths. This is consistent with the experimental observation. The ground state dipole moments of both molecules are equal and are consistent with the reported value of CAM [34]. The results show that the dipole moment of the S_1 state of ACAM is almost equal to that of the ground state. However, the dipole moments of the S_2 (^1L_a) and S_3 states of ACAM are much higher as compared to those of CAM.

4. Discussion

4.1. Nature of the electronic states of ACAM

It has been shown that the replacement of a ring carbon by a nitrogen atom has little or no effect on the π-electronic energy levels of naphthalene [38,39]. That is, the absorption spectral characteristics of quinoline are closely related to that of naphthalene, the long-wavelength band of which consists of ^1L_a and ^1L_b transitions. In naphthalene or quinoline, the energy gap between the transitions is $\sim 3400\ cm^{-1}$. In CAM, due to extended conjugation of the quinoline ring, the four rings (rings A–D) are planar in the molecule. This results in a red shift of the ^1L_b transition with respect to that of quinoline [40–43] without significantly affecting the ^1L_a transition and thus increases the energy gap between the ^1L_a and ^1L_b states. The $-NH_2$ substitution at the 1- or 5-position of naphthalene and quinoline ring respectively causes mixing of the ^1L_a and ^1L_b states of naphthalene and the transition involving the lone-pair electrons on the amine nitrogen, designated $1 \rightarrow \pi^*$ by Kasha and Rawls [44]. As a result, the lowest energy excited states of 1-aminonaphthalene [45,46] and 5-aminoquinoline [47–50] have CT character. Theoretical calculations have also predicted that the lowest energy excited states of aminonaphthalenes have significant CT character; this is particularly true for the S_2 (^1L_a) state of 1-aminonaphthalene [45,46]. Because of the difference in electron distribution in the two excited states, a substituent at the 1-position of naphthalene will interact more effectively with the ^1L_a excited state than the ^1L_b state. This interaction results in a smaller energy separation between the ^1L_a and ^1L_b states compared to that in naphthalene, with ^1L_b still remaining as the lowest excited state [51,52]. In 5-aminoquinoline, the energy gap is expected to be lower as compared to 1-aminonaphthalene ($1400\ cm^{-1}$) because of the enhanced degree of charge transfer from the amine group to the aromatic ring. The same is also true in the case of ACAM. Thus, the absorption band at ~ 335 nm which is far red-shifted compared to that of CAM (~ 290 nm) can be assigned to the ^1L_a transition. Due to symmetry forbiddenness, the intensity of the ^1L_a transition is very weak in CAM. The disappearance of the band upon protonation at the $-NH_2$ group clearly suggests that the transition involved is CT in nature. The large red shift of the short-wave transition in ACAM, relative to that of CAM, suggests that the molecular orbitals involved in the transition are localized in the benzene ring and the transition is polarized along the short axis of the molecule. The red shift of the LW absorption bands in protic solvents is due to the hydrogen-bonding interaction of the solvent molecules with the lone-pair electrons on the ring nitrogen. This suggests that the ^1L_b transition is $\pi \rightarrow \pi^*$ type.

4.2. Dual fluorescence

The dissimilarity between the fluorescence excitation spectra corresponding to the SW and LW emission bands suggests the presence of a trace amount of CAM as impurity in the sample. This is also indicated by the τ_f value of the long-lived decay component of the SW fluorescence which is similar to that reported for CAM in the literature [25]. However, the level of impurity seems to be very low. The appearance of the CAM emission is only due to its very high fluorescence quantum yield (>0.5) [25] compared to ACAM. Thus, the appearance of this small impurity fluorescence does not affect the results of this study, except for the Φ_f values in more polar and protic solvents where the LW fluorescence is weak as compared to the SW fluorescence. In nonpolar solvents (e.g., dioxane, chloroform, etc.), since the fluorescence intensity of the LW band is much higher relative to the SW band, this does not introduce more than 10% error in the measured Φ_f values of ACAM. In more polar and protic solvents, the error in the Φ_f values might be as large as 50%. However, a relative trend can be observed in the Φ_f values of ACAM in various solvents.

Although the SW emission is mainly due to presence of CAM as impurity, the possibility of the appearance of a second emission band at short-wavelengths originating from locally excited ^1L_b state (LE) of ACAM can not be ruled out. The position of the emission maximum of SW band of ACAM is expected to be red-shifted relative to that of CAM. In fact, this is indicated by the fluorescence spectral profile in cyclohexane solvent. The existence of a short-lived decay component corresponding to the SW emission may also suggest the presence of a SW fluorescence originating from the LE state of the molecule. Also, in aqueous solution, a new emission band rises at low pH (2.0) upon protonation at the $-NH_2$ group. This band is red-shifted ($\lambda_{max} = 465$ nm) relative to that of the neutral form of CAM ($\lambda_{max} = 428$ nm) in the same solvent [53]. Usually, in aromatic amines such as aminonaphthalenes, the protonation at the amine group causes both absorption and fluorescence spectra to shift toward higher energy. The resulting spectra resemble the corresponding spectrum of the parent hydrocarbon. Therefore, the new SW fluorescence band can be associated with the emission originating from the LE state of the protonated species (monocation) ACAM. In neutral solvents, the emission from the LE state of ACAM seems to be very weak in intensity as compared to the LW band and therefore, it is lost under the strong impurity fluorescence due to CAM. It seems that the molecule is initially excited to the ^1L_b state and then partially depopulated via internal conversion to the ^1L_a state,

thus giving rise to dual emissions. This explains the low τ_f value of the emission from the LE state as compared to that of CAM. The absence of the short-lived decay component corresponding to the SW band in water suggests that in strong hydrogen-bonding solvents such as water, the SW fluorescence of ACAM is completely quenched by the solvent molecules. This is probably due to the fluorophore-solvent specific interactions involving intermolecular hydrogen bonding. This has been discussed further below.

4.3. Charge-transfer fluorescence and solvent effects

The solvent dependence of the fluorescence spectra of ACAM can be explained in light of the above discussion. The large red shift as well as quenching of the LW fluorescence band in polar solvents suggests that the emitting state is CT type. This is indicted by the large increase in dipole moment ($\Delta\mu = 15$ D) upon excitation. As originally suggested for aminonaphthalenes by Mataga [45] and Suzuki et al. [46], the increase in dipole moment is caused by a change in the electronic configuration of the amino group from tetrahedral (sp^3) in S_o to trigonal (sp^2) in the equilibrium excited state, S_1. The theoretical calculations in Ref. [45] suggest that an excited-state reorganization of the amino group, from the pyramidal to the trigonal structure would increase the CT character primarily of the S_2 (^1L_a) state. Such a relatively minor reorganization resulting in a more polar excited state, could be stabilized by small-amplitude motions in the host solvent, and may thus explain the red shift in the fluorescence spectrum that is observed in cyclohexane, where solute–solvent relaxation (SSR) is restricted. It can be noted that a substantial part of the red shift observed for ACAM in acetonitrile at room temperature is also observable in cyclohexane ($\lambda_{max} = 480$ nm) where SSR is absent. This suggests that the emitting state is a CT state arising from electronic reorganization. According to the discussion in the preceding paragraph, the ^1L_a state of ACAM will be more polar than ^1L_b state. Therefore, in polar solvent, the major polar interaction involves the ^1L_a state and thus have lower energy than the ^1L_b state. Since the so-called ^1L_a transition is no longer a strong $\pi \rightarrow \pi^*$ transition, the large amount of CT character reduces its transition moment (**M**), the magnitude of which increases with solvent polarity after the inversion. Also, lowering of energy of the ^1L_a state in polar solvents decreases the singlet–triplet (S–T) energy gap, thus increasing the probability of intersystem crossing. This explains the decrease of fluorescence quantum yield and lifetime upon increase of solvent polarity.

4.4. Fluorescence quenching

In our recent report on fluorescence properties of CAM in organic solvents, we have demonstrated that the fluorescence intensity of the drug in tetrahydrofuran increases upon addition of water as a result of hydrogen-bonding interaction with the lone-pair electrons on the ring nitrogen [25]. However, in contrast to CAM, we have noted a decrease of intensity of the LW emission in the case of ACAM. This may be attributed to the difference in the nature of the emitting states of the molecules in question. The linearity of the S–V plots (Fig. 10, Fig. 11) clearly suggests that the quenching of CT fluorescence in the presence of protic solvents is due dynamic (collisional) interactions between the fluorophore and the quencher molecules. As suggested by the data in Fig. 12 the quenching of the CT fluorescence of ACAM is linearly related to the hydrogen-bonding strength of the solvent. Although the hydrogen-bonding interactions with the –C=O groups of the pyridone and lactone rings can not be ruled out, such interactions seem to have no significant effect on the fluorescence properties of ACAM as no fluorescence quenching was observed in the case of the parent drug, CAM in hydrogen-bonding solvents. Therefore, the quenching of CT fluorescence must involve the exocyclic amine and ring nitrogen atoms. In the case of CAM, the hydrogen-bonding interaction of solvent molecules with the quinoline nitrogen destabilizes the closely spaced higher energy $^1(n,\pi^*)$ state, thereby decreasing the S–T interaction and thus increasing fluorescence quantum yield [25]. However, such interactions facilitate the charge transfer from the $-NH_2$ group to the partially positively charged hydrogen-bonded ring nitrogen of ACAM which stabilizes the CT state as indicated by the red shift of the spectrum in the presence of hydrogen-bonding solvents (see Table 3). This results in a stronger S–T interaction and hence a decrease of fluorescence quantum yield. In the case of ACAM, a second type of hydrogen-bonding interaction, where the amino lone-pair acts as the donor is also possible. Usually, the hydrogen-bonding interactions of the solvent molecules with the $-NH_2$ group of aromatic amines enhances molecular fluorescence as a result of destabilization of the CT state thus reducing the CT character of the emitting $^1(\pi,\pi^*)$ state. For the same reason, the fluorescence emission from the CT state is quenched in protic solvents. The fluorescence quenching of ACAM in hydrogen-bonding solvents can also be explained using the same principles. Thus, both types of hydrogen-bonding interactions cause fluorescence quenching of ACAM in protic solvents. However, the hydrogen-bonding interaction of the solvent molecules with the $-NH_2$ group is expected to be weaker in the excited state than in the ground state [54]. This is because the $-NH_2$ group and the ring nitrogen atom of aromatic heterocyclics are respectively known to become less and more basic in the excited state [55]. Therefore, the ring nitrogen forms stronger hydrogen bonds with hydrogen-bonding solvents in the excited state as compared to the $-NH_2$ group. The disappearance of the SW emission of ACAM in neutral water clearly suggests that strong hydrogen-bonding interaction of the water molecules with the quinoline lone-pair electrons quenches the SW fluorescence of ACAM. Thus, the quenching of the CT fluorescence of ACAM involves hydrogen-bonding interactions at both nitrogen centers whereas the quenching of the SW emission is due only to the hydrogen-bonding interaction with the ring nitrogen.

It is interesting to note that in contrast to CAM the hydrogen-bonding interaction with the ring nitrogen quenches the fluorescence from the LE state of ACAM.

5. Conclusions

The introduction of the $-NH_2$ group at the 9-position of CAM dramatically changes the absorption and fluorescence behavior of the parent drug. This has been utilized to locate the position of the ^1L_a band ($\sim$335 nm) in the absorption spectrum of ACAM. The fluorescence spectrum of ACAM exhibits dual emission bands originating from both ^1L_a and ^1L_b states. The solvent effects suggest that the emitting state corresponding to the LW emission of ACAM is CT in nature. The CT state is formed after excitation that is stabilized by intramolecular reorganization and polar solute–solvent relaxation about the initially excited ^1L_b state. This involves solute–solvent dipole–dipole reorientation of the polar solvent molecules about the increased (relative to the ground state) dipole moment of the excited ^1L_a state. The spectroscopic evidence suggests that the appropriate label for this new state is ^1L_a/CT. The electronic excitation of the molecule to the CT state involves a large increase in dipole moment. The results of AM1 calculations also suggest that the S_2 state which is the emitting state of the molecule has a large dipole moment. The quenching of the CT emission of ACAM in hydrogen-bond donor solvents is due to dynamic intermolecular hydrogen-bonding interactions between the solvent molecules and the lone-pair-electrons on the amine as well as quinoline nitrogens of the excited molecule. The quenching efficiency increases as the hydrogen-bond-donating capacity of the quencher increases. The solvent sensitive spectral properties of ACAM can be utilized as probes of biological systems to draw conclusions about the site that the probe molecule occupies.

Acknowledgements

The authors acknowledge the National Science Foundation (CHE 9632196) and Department of Energy (DE-FG05-93ER-14367) for partial support of this research. IMW also acknowledges the Philip W. West endowment for partial support of this work. We would like to thank Dr. A. Imondi, Pharmacia, for providing ACAM as a gift.

References

[1] T.G. Burke, A.K. Mishra, M.C. Wani, M.E. Wall, Biochemistry 32 (1993) 5352.
[2] M.E. Wall, M.C. Wani, C.E. Cook, K.H. Palmer, J. Am. Chem. Soc. 88 (1966) 3888.
[3] R.I. Geran, N.H. Greenberg, M.M. MacDonald, A.M. Schumacher, B.J. Abbott, Cancer Chemother. Rep. 3 (1972) 1.
[4] R.E. Perdue Jr., R.L. Smith, M.E. Wall, J.L. Hartwell, B.J. Abbott, Technical Bulletin 1415, Washington, DC, US Department of Agriculture, Agricultural Research Service, April, 1970.
[5] M.E. Wall, Alkaloids with antitumor activity, in: K. Mothes, K. Schreiber, H.R. Schutte (Eds.), International Symposium on Biochemistry and Physiology of the Alkaloids, Academie-Verlag, Berlin, 1969, p. 77.
[6] R.C. Gallo, J. Whang-Peng, R.H. Adamson, J. Natl. Cancer Inst. 46 (1971) 789.
[7] S. Swada, S. Okajima, R. Aiyama, T. Yokokura, K. Yamaguchi, T. Miyasaka, Chem. Pharm. Bull. 39 (1991) 1446.
[8] Y. Kawato, M. Aonuma, Y. Hirota, H. Kuga, K. Sato, Cancer Res. 51 (1991) 4187.
[9] M.C. Wani, A.W. Nicholas, M.E. Wall, J. Med. Chem. 29 (1986) 2358.
[10] M.C. Wani, A.W. Nicholas, G. Manikumar, M.E. Wall, J. Med. Chem. 30 (1987) 1774.
[11] C. Jaxel, K.W. Kohn, M.C. Wani, M.E. Wall, Y. Pommier, Cancer Res. 49 (1989) 1465.
[12] Y.-H. Hsiang, L.F. Liu, M.E. Wall, M.C. Wani, A.W. Nicholas, G. Manikumar, S. Kirschenbaum, R. Silber, M. Potmesil, Cancer Res. 49 (1989) 4385.
[13] R.P. Hertzberg, M.J. Caranfa, S.M. Hecht, Biochemistry 29 (1989) 4629.
[14] Y.-H. Hsiang, M.G. Lihou, L.F. Liu, Cancer Res. 49 (1989) 5077.
[15] M.A. Bjornsti, P. Benedetti, G.A. Vigliani, J.C. Wang, Cancer Res. 49 (1989) 6318.
[16] W.K. Eng, L. Fancette, R.K. Johnson, R. Sternglanz, Mol. Pharmacol. 34 (1988) 755.
[17] W.J. Slichenmyer, E.K. Rowinsky, R.C. Donehower, S.H. Kaufman, J. Natl. Cancer Inst. 85 (1993) 271.
[18] M. Potmesil, Cancer Res. 54 (1994) 1431.
[19] T.G. Burke, A.E. Stanbus, A.K. Mishra, J. Am. Chem. Soc. 114 (1992) 8318.
[20] T.G. Burke, Z. Mi, Anal. Biochem. 212 (1993) 285.
[21] T.G. Burke, Z. Mi, J. Med. Chem. 36 (1993) 2580.
[22] T.G. Burke, Z. Mi, J. Med. Chem. 37 (1994) 40.
[23] Z. Mi, T.G. Burke, Biochemistry 33 (1994) 10325.
[24] Z. Mi, T.G. Burke, Biochemistry 33 (1994) 12540.
[25] J. Dey, I.M. Warner, J. Lumin. 71 (1997) 105.
[26] J. Dey, Warner, J. Photochem. Photobiol. A Chem. 101 (1996) 21.
[27] C.A. Parker, W.T. Rees, Analyst 85 (1960) 587.
[28] W.H. Melhuish, J. Phys. Chem. 65 (1961) 229.
[29] S.R. Meach, D.J. Phillips, Photochem. 23 (1983) 193.
[30] M.J.S. Dewar, E.G. Zoebisch, E.F. Healy, J.P. Stewart, J. Am. Chem. Soc. 107 (1985) 3902.
[31] D.R. Lide (Ed.), CRC Handbook of Chemistry and Physics, 71st edn., CRC Press, Boca Raton, FL, 1990.
[32] E.Z. Lippert, Naturforschung 10A (1955) 5412.
[33] N. Mataga, Y. Kaifu, M. Koizumi, Bull. Chem. Soc. Jpn. 29 (1956) 465.
[34] R.L. Flurry Jr., J.C. Howland, Abstracts, 162 National Meeting of the American Chemical Society, Washington, DC, 1971, No. MEDI-30.
[35] C. Reichardt, Solvents and Solvent Effects in Organic Chemistry, VCH, New York, 1988, p. 378.
[36] M.J.S. Dewar, E.G. Zoebisch, E.F. Healy, J.P. Stewart, J. Am. Chem. Soc. 107 (1985) 3902.
[37] N. Allinger, J. Am. Chem. Soc. 99 (1977) 8127.
[38] D.P. Craig, L.N. Short, J. Chem. Soc. (1945) 419.
[39] J.N. Murrell, The Theory of the Electronic Spectra of Organic Molecules, Methuen, London, 1963, p. 197.
[40] A. Albert, D.J. Brown, G. Cheeseman, J. Chem. Soc. (1951) 474.
[41] E.A. Steck, G.W. Ewing, J. Am. Chem. Soc. 70 (1948) 3397.
[42] M. Godfry, J.N. Murrell, Proc. R. Soc. London, Ser. A 278 (1964) 57.
[43] C.J. Seliskar, L. Brand, J. Am. Chem. Soc. 93 (1971) 5405.
[44] M. Kasha, R.R. Rawls, Photochem. Photobiol. 7 (1968) 561.

[45] N. Mataga, Bull. Chem. Soc. Jpn. 36 (1963) 654.
[46] S. Suzuki, T. Fujii, H. Baba, J. Mol. Spectrosc. 47 (1973) 243.
[47] S.G. Schulman, L.B. Sanders, Anal. Chim. Acta 56 (1971) 83.
[48] E.A. Steck, F.C. Nachod, Z. Phys. Chem. 15 (1958) 372.
[49] E.V. Brown, A.C. Plasz, J. Heterocycl. Chem. 7 (1970) 335.
[50] S.G. Schulman, J. Pharm. Sci. 6 (1971) 371.
[51] K. Nishimoto, R. Fujishiro, Bull. Chem. Soc. Jpn. 37 (1964) 1660.
[52] K. Nishimoto, Bull. Chem. Soc. Jpn. 39 (1966) 645.
[53] J. Dey, I.M. Warner, J. Photochem. Photobiol. A Chem., submitted.
[54] N. Mataga, T. Kubota, Molecular Interactions and Electronic Spectra, Marcel Dekker, New York, 1970.
[55] A. Weller, Progr. Reaction Kinetics 1 (1961) 189.